Marine Geophysical Research (2019) 40:571–579
https://doi.org/10.1007/s11001-019-09387-5

ORIGINAL RESEARCH PAPER

Geoacoustic provinces of the northern South China Sea based on sound speed as predicted from sediment grain sizes

Yuhang Tian[1,2] · Zhong Chen[1] · Zhengyu Hou[1] · Yun Luo[1,2] · Antao Xu[1,2] · Wen Yan[1,2]

Received: 6 August 2018 / Accepted: 23 April 2019 / Published online: 30 April 2019

Abstract

The determination of geoacoustic provinces has important applications in assessing the responses of sedimentary environment and processes. Suitable geoacoustic provinces have not yet been identified in the northern South China Sea, which is an excellent study site for examining sediment acoustic properties. To determine the geoacoustic provinces of sediments in the northern South China Sea, 270 position samples were collected and analysed. Two-parameter empirical equations linking sediment grain-size components to sound speed were applied to sediments from the continental shelf and slope to accurately calculate sound speed in seafloor sediments, especially in the absence of site-specific acoustic data. Based on the ratios of sound speed within the sediments, two geoacoustic provinces are identified. Province I, which is characterized by low sound speed, primarily consists of fine-grained sediments discharged from the Pearl River. Province II, which is characterized by high sound speed, can be further divided into Province II-A and Province II-B. Province II-A is composed of mixed modern and relict sediments originating from the Pearl River and the southwest coast of Taiwan during a Pleistocene drop in sea level. Province II-B consists of coarser relict sediments caused by sea level change during the late Quaternary.

Keywords Grain-size components · Sound speed · Geoacoustic provinces · Seafloor sediments · Northern South China Sea

Introduction

The geoacoustic properties of seafloor sediments can provide basic information for use in ocean engineering, submarine geomorphology and marine geological engineering (Hamilton 1970; Hamilton and Bachman 1982; Wang et al. 2016; Ballentine et al. 2017; Kan et al. 2017). Previous studies have attempted to develop quantitative relationships between the physical and acoustic properties of seafloor sediments from different areas (Buckingham 1998; Zheng et al. 2016; Kim et al. 2017; Hou et al. 2018a, b), which are the basis for proposed geoacoustic models (Wilson 1960; Hamilton 1980; Buckingham 1997; Stoll et al. 1998; Chotiros and Isakson 2004; Lu et al. 2006; Li et al. 2009; Kimura 2011; Zou et al. 2011). The physical and acoustic properties in all areas can be partly estimated using a geoacoustic model suggested by Hamilton (Kim et al. 2012; Bae et al. 2014). However, it is still difficult to represent the acoustic characteristic of all areas completely given their diverse sedimentary environment (Kim et al. 2017). Thus, it is necessary to identify geoacoustic provinces that accurately reflect the sedimentary environments before establishing a geoacoustic model.

Investigations of geoacoustic provinces have been conducted in many marine regions (Kim et al. 2011, 2012). For example, Kim et al. (2011) identified three geoacoustic provinces in the South Sea shelf of Korea based on sediment properties related to sediment sources and sea level change. Based on the empirical relationships between mean grain size and sound speed proposed by Hamilton, Kim et al. (2012) subsequently revised that analysis and identified four geoacoustic provinces in the same region. Using new empirical equations based on the physical properties and textures of sediments, as well as corrections for the compressional wave speed based on in situ temperatures and pressures, Kim et al. (2017) have more recently identified four geoacoustic provinces in the Ulleung Basin in the Korean East Sea.

In the South China Sea (SCS), many studies have focused on revealing relationships between the physical and acoustic

✉ Zhong Chen
chzhsouth@scsio.ac.cn

[1] CAS Key Laboratory of Ocean and Marginal Sea Geology, South China Sea Institute of Oceanology, Chinese Academy of Sciences, Guangzhou 510301, China

[2] University of Chinese Academy of Sciences, Beijing 100049, China

properties of sediments. However, only a handful of studies have attempted to identify geoacoustic provinces within the SCS. For example, studies conducted near Hainan Island have reported the occurrence of high- and low-sound-speed sediments (Lu et al. 2007; Tian et al. 2016), and in those two studies, the high- and low-sound-speeds for sediments are defined to be greater and less than 1530 m/s (approximately the speed in seawater), respectively. Wang et al. (2016) identified three geoacoustic provinces in the southern SCS and determined that the sound-speed ratio distribution is closely related to physical properties of the sediments. Hou et al. (2018a, b) also identified three geoacoustic provinces in the central basin on the basis of sediment properties. Nevertheless, these studies do not provide the distribution of geoacoustic provinces in the northern SCS.

In this study, we suggest new empirical equations based on samples from the continental shelf and the continental slope in the northern SCS. Furthermore, we define a series of geoacoustic provinces in the study area using the ratio of the sound speed of sediment to the sound speed of water in the standard laboratory conditions. The results of this study are useful in predicting marine engineering properties and developing a high-resolution geoacoustic model.

Regional setting

The study area is located in the northern South China Sea, and is surrounded by mainland China, Taiwan, Luzon and Hainan Island. In the northern SCS, sediment sources include the Pearl River, southwestern Taiwan and the Luzon arc system, which provide large amounts of terrestrial sediment to the study area (Liu et al. 2010a, b, 2008a, b). Most of the sediments are deposited on the continental shelf, but a small amount is transported further and deposited in the abyssal basin (Liu et al. 2011). The study area is usually divided into the continental shelf and the continental slope. The inner shelf is dominated by clayey silt, while the outer shelf is dominated by silty sand and sandy silt (Pan 2003). Gas hydrates have been documented on the continental slope, but are likely absent on the continental shelf (Wang et al. 2018). The continental slope is mainly covered by silty clay and clayey silt (Luo et al. 1994) (Fig. 1).

Materials and methods

The data analysed in this study area (17–24°N and 109–121.5°E) were collected from 270 stations (Fig. 1). We also compiled literature data on sediment sound speed comprising 139 data points (Lu et al. 2005; Pan 2003). For the northern SCS, we obtained the sound speeds and grain-size components distribution from 48 sites on the continental shelf and continental slope. Additionally, grain-size components have been measured for 83 samples collected by the South China Sea Institute of Oceanology of the Chinese Academy of Sciences over the past 10 years.

A box corer was used to collect 48 sediment samples. After the seafloor sediments were collected, we inserted PVC tubes into the box corer to collect short cylindrical samples, each of which was approximately 0.3–0.5 m long. Compressional sound speed was measured in a standard laboratory (23 °C, atmospheric pressure) by applying the coaxial differential distance method using a portable WSD-3 digital sonic instrument (Hou et al. 2015). The acoustic transducers were in direct contact with top of the sediment core and were coupled to the liner on the bottom

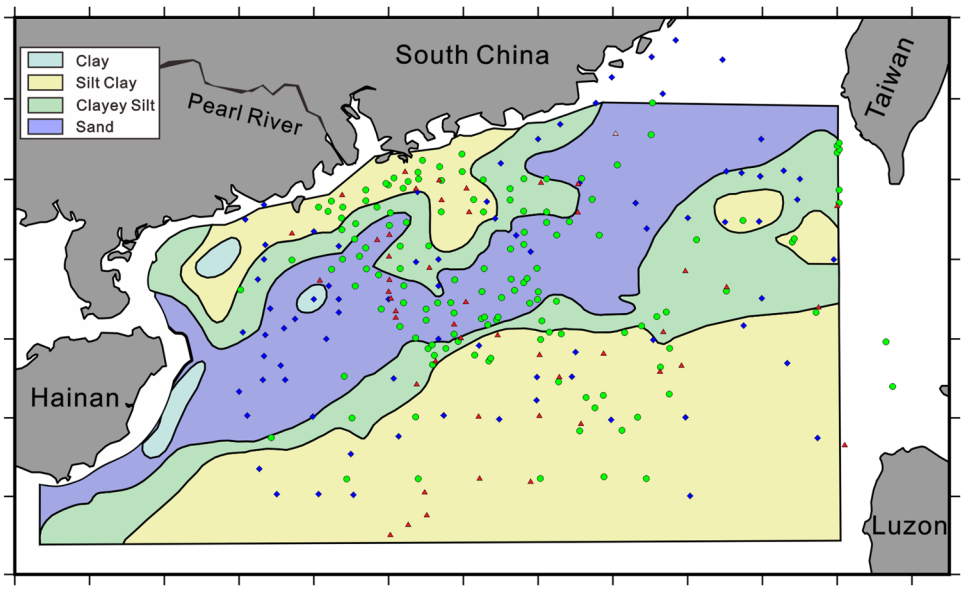

Fig. 1 Locations of samples and sediment type distribution in this study (modified from Liu et al. 2011). The circle data points (sound speed samples) are from Pan (2003) and Lu et al. (2005), the triangle data points (sound speed and grain-size samples) and the diamond data points (grain-size samples) represent samples collected by the South China Sea Institute of Oceanology of the Chinese Academy of Sciences

by using Vaseline (Fig. 2). The centre frequency of the pulse signal was 100 kHz, the sound wave sampling length was 4096 points, the length measurement accuracy of the sediments cylindrical sample was 0.5 mm, the transducer-calibrated time is t_0, the signal sampling interval was 0.1 μs. The sound speed (v_p) was calculated as follows:

$$v_p = \frac{L_0}{t - t_0}$$

where L_0 is the length of the cylindrical sediment sample, t is the propagation time of the compressional wave, and t_0 is the transducer-calibrated time.

The calculation of uncertainty was performed using statistical methods and the accuracy calculation method is as follows (Hou et al. 2018a, b):

$$\Delta A = S_x = \sqrt{\sum (x_i - x)^2 / n}$$

The equation is used for repeated measurement and the uncertainty of the sound speed measurements is approximately ± 5 m/s. S_x is the variance value, x_i is the measured value, x is the average value, and the n is the number of measurements.

Seawater speed (V_0) is an important parameter and can be expressed as a function of temperature (T), salinity (S), and depth (Z). Wilson (1960) derived the formula of seawater speed:

$$V_0 = 1449.2 + 4.6T - 0.055T^2 + (1.34 - 0.010T)(S - 35) + 0.016Z$$

The surficial seawater speed was reported for the standard laboratory conditions favoured by Hamilton (23 °C, 35 ppt, and atmospheric pressure). These conditions correspond to a water sound speed of 1529.97 m/s.

The grain-size components were analysed using a laser particle sizer (Malvern Mastersizer 2000) at the South China Sea Institute of Oceanology of the Chinese Academy of Sciences. Sediment samples were separated into two groups based on the range of grain sizes (0.02–2000 μm) for which measurements with the laser particle sizer can be made. Samples with particle grain sizes entirely within this range were measured directly, while samples with coarse particles (> 2000 μm) were sieved using a 1 mm mesh sieve. The fraction above the sieve was analysed using standard sieving methods, while the fraction below the sieve was measured directly using the laser particle sizer. Grain-size data for the two fractions were then combined using the Mastersizers2000 simulation program. Triplicate analyses were performed on each sample. The mean values of each parameter were then calculated; the associated standard deviations were < 3%.

For sites where grain-size components data were collected but no sound-speed data were available, sound speed was estimated using the empirical equations presented later in this study. Based on the different depositional environments, we propose different empirical equations for the continental shelf and slope areas of the northern SCS. The sound-speed ratio, important for distinguishing geoacoustic provinces, is based on the ratio of the sound speed of sediment to the sound speed of water in the standard laboratory conditions, not to the sound speed of the in situ surficial seawater.

Results

The empirical equations linking sediment grain-size components were proposed for the continental shelf and slope to accurately calculate sound speed, especially in the absence in the range of site-specific acoustic data. The measured and calculated speeds showed a great amount of variation of 1459–1814 m/s (average 1592 m/s) on the continent shelf, and 1418–1744 m/s (average 1491 m/s) on the continent slope. The average sound speed on the continental shelf is

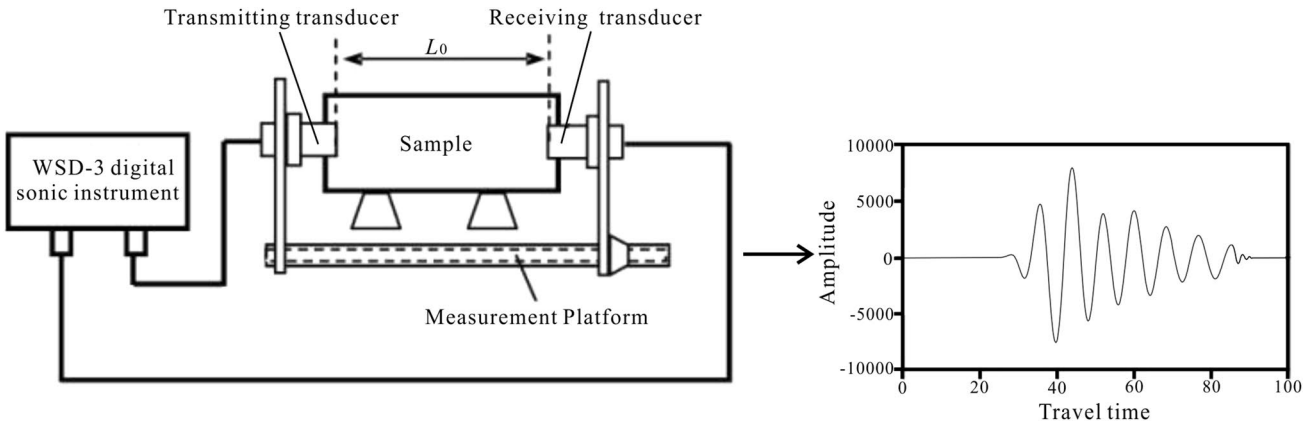

Fig. 2 Schematic of a WSD-3 sonic instrument to measure the sound speed in sediments

higher by up to 101 m/s than that on the continent slope. The sound speed of sediments on the continental slope is significantly lower than that of sediments on the continental shelf (Fig. 3). The distribution patterns of the surficial sediment sound speeds are in good agreement with the marine geological characteristics in the continental shelf and slope environment.

Based on the ratios of sound speed within the sediments, the geoacoustic provinces in the study area can be divided into two provinces: Province I, which is characterized by low sound speed; Province II, which is characterized by high sound speed, can be further divided into Province II-A and Province II-B. The sound speed and grain-size components for each province are given in Table 1. The sound speeds in Province I vary between 1418 m/s and 1529 m/s, while those in Province II vary between 1530 m/s and 1814 m/s. The low sound-speed province (Province I) mainly consists of clayey silt. In the high sound-speed province (Province II), the sediments are dominated by sandy silt and silty sand.

Discussion

Relationships between sound speed and grain-size components

Many studies have demonstrated that grain-size composition is an important parameter from which to predict sediment sound speed (Hamilton et al. 1955). Additionally, Hamilton (1970) suggested that some sediment textural properties, for example whether sediments are originally wet or dry, are among the best indices from which to derive empirical equations of sediment sound speed. Irrespective of the sedimentary environment, percentages of sand, silt, and clay are generally better indices of sediment sound speed than porosity and density (Neto et al. 2011; Kim 2001; Goff et al. 2004; Wang et al. 2016).

From the perspective of many researchers, the distribution of sediment geoacoustic properties is related to the sedimentary environment (Hamilton 1970; Briggs and Fischer 1991; Kim et al. 2017). To accurately estimate the geoacoustic properties of marine sediments, it is necessary to establish geoacoustic models that accurately reflect the geoacoustic properties of each sedimentary environment.

Generally, the continental slope area is covered by fine-grained sediments, while the continental shelf is covered by

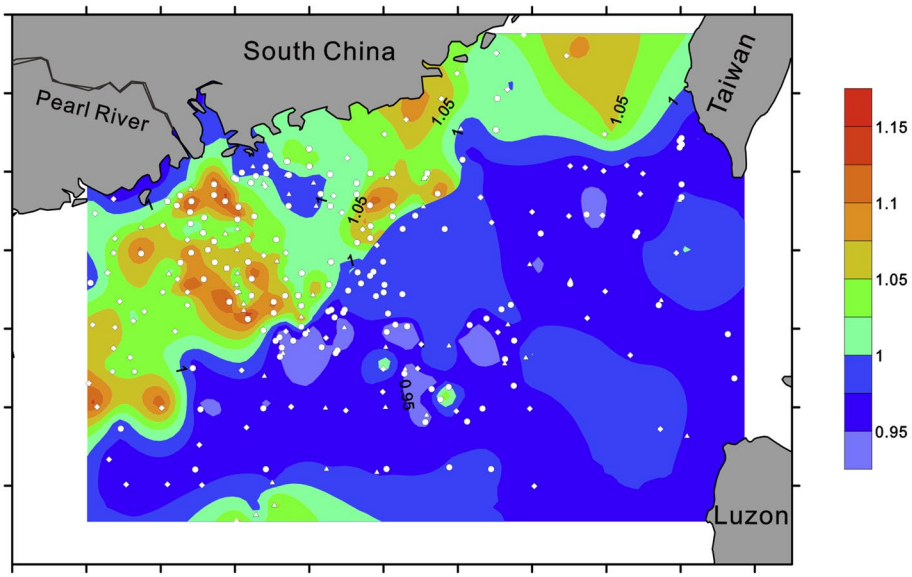

Fig. 3 Spatial distribution of the sediment measured and calculated sound speed. The circular and the triangle points represent samples measured and the diamond points represent samples calculated

Table 1 Sound-speed and grain-size components for the geoacoustic provinces identified in this study

Province	V_p (m/s)		Sand (%)	Silt (%)	Clay (%)	Sediment type
	Range	Average				
I	1418–1529	1478	6.67	61.99	31.34	Clayey silt
II-A	1530–1599	1564	32.64	49.45	17.92	Sandy silt
II-B	1600–1814	1661	63.81	26.41	9.79	Silty sand

coarse-grained sediments (Liu et al. 2011). Based on this division, empirical equations relating sound speed to grain-size compositions in different regions are established in this work.

The empirical equations for Northern SCS (i.e., Eqs. 1–6) are matched from the grain-size components and sound speed at the 48 sites on the continental shelf and continental slope. 23 of the 48 sites are located on the continental shelf, and the grain-size components and sound speed at these 23 sites are used to fit the empirical equations for the continental shelf (i.e., Eqs. 7–12). The other 25 sites are situated at the continental slope, and their grain-size components and sound speed construct the empirical equations for continental slope (i.e., Eqs. 13–18). Table 2 displays the range of our measured sound speed and content of sand, silt and clay at the 48 sites.

Based on the empirical equations presented in Table 3, we can see that the maximum R^2 values for the northern SCS, continental shelf, and continental slope are 0.72, 0.81, and 0.83, respectively. Hence, the sound-speed equations for the continental shelf and slope exhibit larger R^2 values than the corresponding equations for the northern SCS. Furthermore, the R^2 values of the two-parameter equations are greater than the R^2 values of the single-parameter equations. Based on this analysis, we determine that the two-parameter equations connecting sediment sound speed and grain size composition (sand and clay) are best suited to this particular study area. Therefore, we calculate the expected sound speed using the two-parameter Eqs. 11 and 17 (Fig. 4).

Many empirical equations between sound speed and grain size composition have been established for different marine regions. To analyse the accuracy of the equations proposed by these studies, we used the literature equations presented in Table 4 to calculate the expected sound speeds for sediments collected from our study area. Through this calculation, we find that the mean relative errors (MRE) of the empirical equations are less than 4 percent. Furthermore, we see that the MRE of the equations developed in this study for the continental shelf and continental slope are lower than those of the equations collected from the literature, indicating that the empirical equations of sediment sound speed developed in this study are suitable for predicting the sound speeds of seafloor sediments within our study area.

Table 2 The range of our measured sound speed and content of sand, silt and clay at the 48 sites for each different region

Region	V_p (m/s)	Sand (%)	Silt (%)	Clay (%)
Northern SCS	1440–1660	0.05–85.97	10.85–72.95	3.18–41.97
Continental shelf	1500–1660	1.09–85.97	10.85–72.48	3.18–34.57
Continental slope	1440–1630	0.05–43.70	40.34–72.95	12.74–41.96

Table 3 Empirical equations of the sound speed and grain-size components for each different region

Region	Empirical equation	R^2	No.
Northern SCS	$v_p = 1534 + 56.89S - 7.471S^2$	0.66	1
	$v_p = 1521 - 33.44T + 6.028T^2$	0.47	2
	$v_p = 1521 - 45.72C + 6.373C^2$	0.64	3
	$v_p = 2337 - 8.812S - 29.18T + 0.022S^2 + 0.210ST + 0.242T^2$	0.72	4
	$v_p = 1839 - 7.095\mathrm{S} - 19.23\mathrm{C} + 0.055S^2 + 0.275SC + 0.242C^2$	0.71	5
	$v_p = 1677 - 3.838T + 4.394C + 0.055T^2 - 0.165TC + 0.022C^2$	0.71	6
Continental shelf	$v_p = 1476 - 1.505S + 0.129S^2$	0.75	7
	$v_p = 2860 - 42.96T + 0.331T^2$	0.61	8
	$v_p = 1936 - 28.74C + 0.426C^2$	0.73	9
	$v_p = 2433 - 34.59S - 28.31T + 0.351S^2 + 0.479ST + 0.209T^2$	0.80	10
	$v_p = 1693 - 0.225S - 13.50C + 0.082S^2 - 0.061SC + 0.209C^2$	0.81	11
	$v_p = 2489 - 16.14T - 35.70C + 0.082T^2 + 0.224TC + 0.352C^2$	0.80	12
Continental slope	$v_p = 1523 + 1.319S$	0.73	13
	$v_p = 1701 - 4.325T + 0.028T^2$	0.67	14
	$v_p = 1638 - 4.76C + 0.036C^2$	0.65	15
	$v_p = 467.6 + 30.27S + 25.89T - 0.181S^2 - 0.370ST - 0.155T^2$	0.82	16
	$v_p = 1511 - 1.657S + 5.03C + 0.034S^2 + 0.060SC - 0.155S^2$	0.83	17
	$v_p = 1683 - 5.097T + 5.965C + 0.034T^2 + 0.007TC - 0.181C^2$	0.82	18

v_p is the sediment sound speed, S is the sand component, T is the silt component, and C is the clay component. R^2 is the coefficient of determination. No. is the reference number of the equation

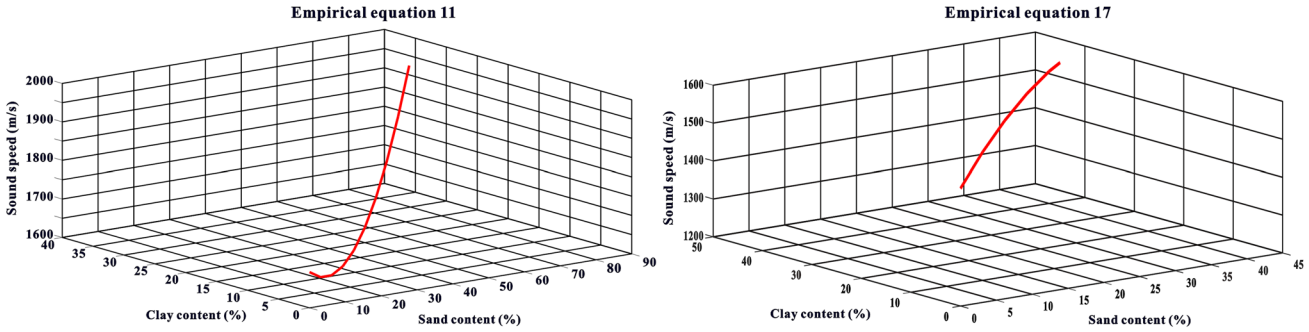

Fig. 4 Relationship between the sand content and clay content versus sound speed of the two-parameter Eqs. 11 and 17

Table 4 Comparison between the empirical equations developed in this study and those obtained from the scientific literature. MRE is the mean relative error

Citation	Empirical equation	MRE (%)
Hamilton (1970)	$v_p = 1513.7 + 2.54S$	2.89
Orsi and Dunn (1991)	$v_p = 1490.1 + 2.288S + 0.00052S^2$	1.99
Meng (2012)	$v_p = 1489.1 + 4.603S - 0.0465S^2$	2.31
Wang (2015)	$v_p = 1489.1 + 1.9703S$	1.91
Wang et al. (2016)	$v_p = 1549.4 - 0.66C$	3.09
This study in shelf	$v_p = 1693 - 0.225S - 13.50C + 0.082S^2 - 0.061SC + 0.209C^2$	0.79
This study in slope	$v_p = 1511 - 1.657S + 5.03C + 0.034S^2 + 0.060SC - 0.155S^2$	1.38

Geoacoustic provinces

Wang et al. (2016) reported the variation of sound-speed ratios in the southern SCS and subsequently identified two sound-speed provinces. He has concluded that the distribution of sound-speed ratios is related to the physical properties (i.e., porosity and density), level of compaction, and consolidation state of the sediments in different sedimentary environments. Additional studies have suggested that a high-speed province should be defined as having a sound-speed ratio > 1, while low-speed provinces should be defined as having a sound-speed ratio < 1. The sound-speed ratio in the study area is calculated both from the observed sound speed data and from the sound speed predicted on the basis of grain-size analyses. Similar to the results of previous studies (Lu et al. 2007; Tian et al. 2016; Wang et al. 2016), we divide the northern SCS into two geoacoustic provinces based on differences in the sound-speed ratios. Province I is characterized by low sound-speed ratios (R < 1) while Province II is characterized by high sound-speed ratios (R > 1). Based on particle size composition, sound-speed ratio, and sedimentary environment, Province II is further divided into Province II-A and Province II-B (Fig. 5).

The spatial distribution of geoacoustic provinces in the study area is shown in Fig. 5. Province I, which exhibits the lowest sediment sound speed, is the largest province in the study area and is distributed both near the mouth of the Pearl River (Province I-1) and on the continental slope (Province I-2) (Fig. 5). The average sediment sound speed in Province I-1 is 1506 m/s, while the average sound speed in Province I-2 is 1471 m/s. Province I-1 is covered with both muddy and sandy sediments supplied directly by the Pearl River, while Province I-2 is covered with muddy sediments.

Province II-A is primarily located on the continental shelf of the northern SCS (Province II-A1) with a small fraction (Province II-A2) distributed near the Paracel Islands (Fig. 5). As shown in Table 1, sediment sound speed range from 1530 to 1599 m/s (average 1564 m/s), and the sediment is mainly sandy silt. Province II-A1, which is composed of Holocene mud and Pleistocene sand (Pan. 2003), exhibits high sediment sound speed relative to Province I. This province is likely determined by both relict deposits and modern deposits originating from the Pearl River and southwest of Taiwan (Pan. 2003, Liu et al. 2008a, b). Based on our sampling analyses, we discovered the small amount biogenic debris in Province II-A2, and the biogenic debris sources are probably primarily from the Paracel Islands.

Province II-B can be divided into Province II-B1, Province II-B2, Province II-B3, and Province II-B4 (Fig. 5). As shown in Table 1, sediment sound speed in Province II-B ranges from 1600 to 1814 m/s (average 1661 m/s), and the dominant sediment type is silty sand (Table 1). Province II-B1 is mainly located on the continent shelf southeast off Hainan Island, and sediment sound speed ranges from 1600 to 1744 m/s. Province II-B2 is distributed on the outer continental shelf off the west of Guangdong Province with the

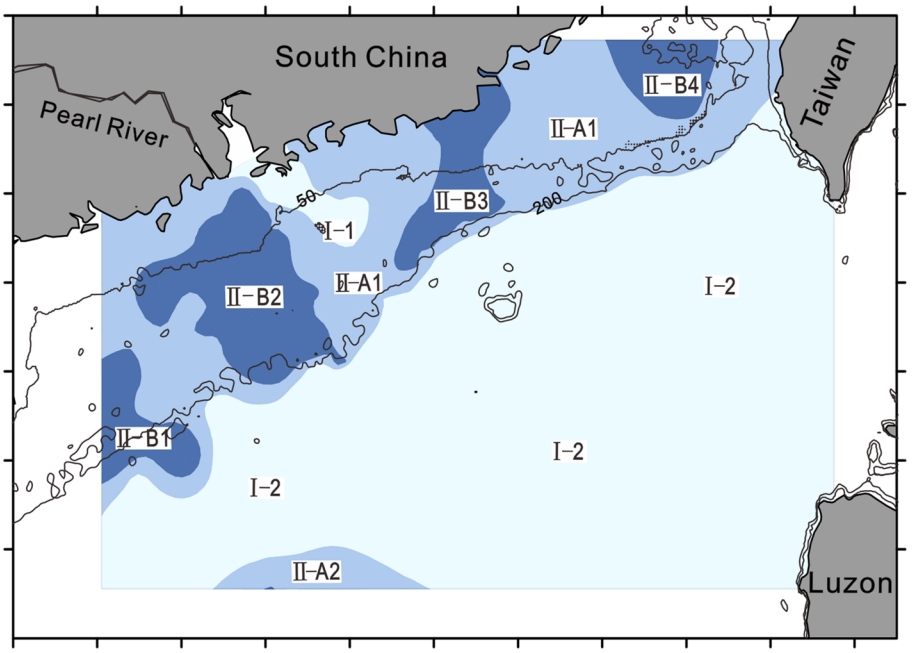

Fig. 5 Geoacoustic provinces (I, IIA, IIB) identified in this study

sediment sound speed ranging from 1600 to 1807 m/s. Similar to the Province II-B2, the sound speed in Province II-B3 shows limited variation in between 1604 and 1814 m/s on the outer continent shelf off the east of Guangdong Province. The sound speed in Province II-B4, located on the continental shelf southwest of Taiwan, ranges from 1604 to1652 m/s.

According to previous analysis, sediments near the mouth of the Pearl River consist of modern deposits (Pan 2003). Clayey silt is the dominant sediment type in Province I-1 and originates primarily from discharge of the Pearl River. In accordance with hydrodynamic gradients, coarse-grained sediments are deposited in the near shore environment, while fine-grained particles are transported and deposited farther away. Surficial sediments on the continent slope, which also belong to Province I-2, are characterized by clayey silt, suggesting that hydrodynamic forces are relatively weak in this environment. Endler et al. (2015) confirmed that finer particle size ranges are typically associated with lower sediment sound speed. Therefore, the fine-grained sediments present near the mouth of the Pearl River and on the continental slope are most likely the cause of the lower sound speed that characterize Province I.

In contrast to Province I, Province II-A is composed of coarse-grained sediments with correspondingly high sound speed. The average sediment sound speed in Province II-A is 86 m/s higher than the average for Province I. Surficial sediments in Province II-A1 most likely originate from discharge of the Pearl River and the southwest coast of Taiwan, transported by a branch of the Kuroshio Current and Guangdong Coastal Current (Liu et al. 2008a, b, 2011; Zhong et al. 2017). The area, with water depth ranging from 30 to 60 m, is a mixed-deposit region formed during a late Quaternary rise in sea level (Pan 2003). Relict deposits that occur in the northern SCS at water depths > 60 m are a result of a drop in sea level during the Pleistocene and are dominated by coarser-grained sand (Pan 2003). Sedimentation in this area is affected by hydrodynamic processes and the accumulation of sediment by the ocean during the postglacial period (Steinke et al. 2003). As a result of these geological processes, surficial sediment types in this area are silt, silty sand, fine sand, and coarse sand. Furthermore, as shown in Fig. 5, Province II-A2 also occurs within the region dominated by Province I. In our studies, we confirm that sediments in Province I are generally characterized by fine particle sizes and low sound speeds. However, based on our field sampling and subsequent analyses, coarse-grained sediments are also present, distributed near seamounts and coral reefs. Overall, the distributions of sediment sound speeds in Province II-A are consistent with the trend linking higher sound speeds to coarser grain sizes.

Compared with Province I and Province II-A, Province II-B exhibits the highest sediment sound speed and most complex sedimentary environment (Fig. 5). As shown in Table 1, sediment sound speeds in Province II-B range from 1600 to 1814 m/s (average = 1661 m/s). Combined with sedimentary environment and sediment sources, Province II-B can be further divided into four areas (e.g., Province II-B1, Province II-B2, Province II-B3, and Province II-B4). Several sediment samples collected in Province II-B1 also exhibit abundant concentrations of biogenic debris. Therefore, Province II-B1 shows the highest sound speed value (average = 1678 m/s) in comparison with the other provinces. The

sediment source in this area is primarily from Hainan Island. Province II-B2, in the northern SCS, has a distinct tongue-shaped pattern extending from the Pearl River estuary to southeastern Hainan Island. The surface sediment sources in Province II-B1 and Province II-B2 primarily come from Hainan Island, transported by surface currents. Driven by the ocean current, the coarse-particle sediments are deposited near shore, and the fine particles are transported a farther distance (Zhong et al. 2017). For the same sediment source, sediment particle size decreases away from the sediment source. Generally, coarse-grained sediment has a higher sound speed. In this study, Province II-B1 is closer to Hainan Island than Province II-B2. Therefore, the sound speeds in Province II-B1 are higher than that in Province II-B2. Form Province II-B2 and Province II-B3, the average sound speed (1662 m/s) in Province II-B2 and that (1664 m/s) in Province II-B3 display excellent symmetry. The sediment source in Province II-B3 is mainly determined by the Pearl River. This province is mostly composed of relict sediments with sand caused by sea level change during the late Quaternary. Province II-B4 lies around the Taiwan Shoal, and is mainly controlled by local topography and currents. Liu and Xia (2004) proposed that the Taiwan Shoal not only consists of relict deposits but also modern deposits. Therefore, Province II-B4 shows the lowest average sound speed (1624 m/s).

Conclusions

(1) This study proposes empirical equations that connect grain-size compositions to sediment sound speed for the continental shelf and slope regions of the northern SCS. These two-parameter equations can be accurately used to predict sediment sound speed, especially in areas where in direct measurements of sound speed are lacking.

(2) Based on the sound-speed ratio of surficial sediments, we divide the northern SCS into two geoacoustic provinces. Low sound-speed ratio ($R < 1$) sediments are designated as Province I, while high sound-speed ratio ($R > 1$) sediments are designated as Province II. Based on particle size composition, sound-speed ratio, and sedimentary environment, geoacoustic Province II is further subdivided into Province II-A and Province II-B.

(3) Geoacoustic provinces can be predicted by the sound-speed ratio which is derived from the sediment grain sizes. Province I hosts fine-grained sediments with low sound speed. Province II is dominated by coarse-grained sediments with correspondingly high sound speed.

Acknowledgements This work has been financially supported by the project of the Chinese National Science Foundation (Contracts 41676056), the Key Laboratory of Marine Mineral Resources, the Ministry of Land and Resources. We thank two anonymous reviewers for their constructive criticisms and vauable suggestions with respect to the presentation of this paper. We appreciate the enthusiastic support of editors for providing language help. We also thank Prof. B. Lu for data collation.

References

Bae SH, Kim DC, Lee GS, Kim GY, Kim SP, Seo YK, Kim JC (2014) Physical and acoustic properties of inner shelf sediments in the South Sea, Korea. Quat Int 344:125–142

Ballentine WM, Dorgan KM, Lee KM, Ballard MS, McNeese AR, Wilson PS, Venegas GR (2017) Effects of marine infauna on the acoustic properties of sediment. J Acoust Soc Am 142(4):2693

Briggs K, Fischer R (1991) Geoacoustic model of the strait of Korea. NOARL Technical note, pp 1–44

Buckingham MJ (1997) Theory of acoustic attenuation, dispersion, and pulse propagation in unconsolidated granular materials including marine sediments. J Acoust Soc Am 102(5):2579–2596

Buckingham MJ (1998) Theory of compressional and shear waves in fluidlike marine sediments. J Acoust Soc Am 103(1):288–299

Chotiros NP, Isakson MJ (2004) A broadband model of sandy ocean sediments: biotStoll with contact squirt flow and shear drag. J Acoust Soc Am 116:2011–2022

Endler M, Endler R, Bobertz B, Leipe T, Arz HW (2015) Linkage between acoustic parameters and seabed sediment properties in the south-western Baltic Sea. Geo Mar Lett 35(2):145–160

Goff JA, Kraft BJ, Mayer LA, Schock SG, Sommerfield CK, Olson HC, Gulick SPS, Nordfjord S (2004) Seabed characterization on the New Jersey middle and outer shelf: correlatability and spatial variability of seafloor sediment properties. Mar Geol 209(1):147–172

Hamilton EL (1970) Sound speed and related properties of marine sediments, North Pacific. J Acoust Soc Am 72:1891–1904

Hamilton EL (1980) Geoacoustic modeling of the sea floor. J Acoust Soc Am 68:1313–1340

Hamilton EL, Bachman RT (1982) Sound speed and related properties of marine sediments. J Acoust Soc Am 72:1891–1904

Hamilton EL, Shumway G, Menard HW, Shipek CJ (1955) Acoustic and other physical properties of shallow-water sediments off san diego. J Acoust Soc Am 28(1):1–15

Hou Z, Guo C, Wang J, Chen W, Fu Y, Li T (2015) Seafloor sediment study from south china sea&58; acoustic & &59; physical property relationship. Remote Sens 7(9):11570–11585

Hou Z, Chen Z, Wang J, Zheng X, Yan W, Tian YH, Luo Y (2018a) Acoustic impedance properties of seafloor sediments off the coast of Southeastern Hainan, South China Sea. J Asian Earth Sci 154:1–7

Hou Z, Chen Z, Wang J, Zheng X, Yan W, Tian Y, Luo Y (2018b) Acoustic characteristics of seafloor sediments in the abyssal areas of the South China Sea. Ocean Eng 156:93–100

Kan G, Liu B, Wang J, Meng X, Li G, Hua Q, Sun L (2017) Sound speed dispersion characteristics of three types of shallow sediments in the southern yellow sea. Mar Georesour Geotechnol 36(7):853–860

Kim GY, Kim DC (2001) Comparison and correlation of physical properties from the plain and slope sediments in the Ulleung Basin, East Sea (Sea of Japan). J Asian Earth Sci 19(5):669–681

Kim GY, Kim DC, Yoo DG, Shin BK (2011) Physical and geoacoustic properties of surface sediments off eastern Geoje Island, South Sea of Korea. Quat Int 230(1–2):21–33

Kim DC, Kim GY, Yi HI, Seo YK, Lee GS, Jung JH, Kim JC (2012) Geoacoustic provinces of the South Sea shelf off Korea. Quat Int 263:139–147

Kim SR, Lee GS, Kim DC, Bae SH, Kim SP (2017) Physical properties and geoacoustic provinces of surficial sediments in the southwestern part of the Ulleung Basin in the East Sea. Quat. Int 459:35–44

Kimura M (2011) Speed dispersion and attenuation in granular marine sediments: Comparison of measurements with predictions using acoustic models. J Acoust Soc Am 129(6):3544–3561

Li GX, Lu B, Huang SJ (2009) Influence of microstructure change of seafloor sediments on the sound speed in them in the course of stress-strain. Mar Sci Bull 11(1):62–69

Liu Z, Xia D (2004) Tidal sands in the China seas. China Ocean Press, Beijing

Liu JP, Liu CS, Xu KH, Milliman JD, Chiu JK, Kao SJ, Lin SW (2008a) Flux and fate of small mountainous rivers derived sediments into the Taiwan Strait. Mar Geol 256:65–76

Liu ZF, Tuo ST, Colin C, Liu JT, Huang CY, Selvaraj K, Chen CTA, Zhao YL, Siringan FP, Boulay S (2008b) Detrital fine-grained sediment contribution from Taiwan to the northern South China Sea and its relation to regional ocean circulation. Mar Geol 255:149–155

Liu JG, Chen Z, Chen MH, Yan W, Xiang R, Tang XZ (2010a) Magnetic susceptibility variations and provenance of surface sediments in the South China Sea. Sediment Geol 230:77–85

Liu JG, Chen Z, Yan W, Chen MH, Yin XB (2010b) Geochemical characteristics of rare earth elements in the fine-grained fraction of surface sediment from South China Sea. Earth Sci. J. China Univ. Geosci 23:563–571

Liu JG, Xiang R, Chen M, Chen Z, Yan W, Liu F (2011) Influence of the Kuroshio current intrusion on depositional environment in the Northern South China Sea: evidence from surface sediment records. Mar Geol 285:59–68

Lu B, Li G, Huang S (2005) The comparing of seabed sediment acoustic-physical properties in the Yellow Sea, the East China Sea and northern the South China Sea. Ocean Technology 24(2):28–33 **(in Chinese with English abstract)**

Lu B, Li G, Huang S, Li C (2006) Physical properties of sediments on the Northern continental shelf of the South China Sea. Mar Georesour Geotechnol 24(1):47–60

Lu B, Li G, Liu Q, Huang S, Zhang F (2007) A study on seafloor sediment and its acouso-physical properties in the southeast offshore sea area of Hainan Island in China. Acta Oceanol Sin 29(4):34–41 **(in Chinese with English abstract)**

Luo YL, Feng WW, Lin HZ (1994) Bottom sediment types and depositional characteristics of sediments of the South China Sea. Trop Oceanol 13:47–54 **(in Chinese with English abstract)**

Meng XM, Liu BH, Kan GM, Li GB (2012) An experimental study on acoustic properties and their influencing factors of marine sediment in the southern Huanghai Sea. Acta Oceanol Sin 34(6):74–83 **(in Chinese with English abstract)**

Neto AA, Teixeira Mendes JDN, de Souza JMG, Redusino M Jr, Leandro Bastos Pontes R (2011) Geotechnical influence on the acoustic properties of marine sediments of the Santos Basin. Brazil Mar Georesourc Geotechnol 31(2):125–136

Orsi TH, Dunn DA (1991) Correlations between sound velocity and related properties of glacio-marine sediments: Barents Sea. Geo-Mar Lett 11(2):79–83

Pan GF (2003) Research on the acoustic characteristics of seabed sediments in the Northern South China Sea. Dissertaion, University of Tongji (**in Chinese with English abstract**)

Steinke S, Kienast M, Hanebuth T (2003) On the significance of sea-level variations and shelf paleo-morphology in governing sedimentation in the southern South China Sea during the last deglaciation. Mar Geol 201(1–3):179–206

Stoll RD, Bautista EO (1998) Using the Biot theory to establish a baseline geoacoustic model for seafloor sediments. Cont Shelf Res 18(14–15):1839–1857

Tian Y, Chen Z, Liu J, Huang W, Zhong Y (2016) Influence of the grain size on the porosity and acoustic speed of offshore surface sediments in the Southeastern Hainan Island. J Trop Oceanogr 35(3):48–54 **(in Chinese with English abstract)**

Wang J (2015) Study of the in situ acoustic measurement technique and geoacoustic properties of marine sediments. Dissertaion, University of Chinese Academy of Sciences (**in Chinese with English abstract**)

Wang J, Guo C, Liu B, Hou Z, Han G (2016) Distribution of geoacoustic properties and related influencing factors of surface sediments in the southern South China Sea. Mar Geophys Res 37(4):337–348

Wang J, Wu S, Yao Y (2018) Quantifying gas hydrate from microbial methane in the South China Sea. J Asian Earth Sci 168:48–56

Wilson WD (1960) Equation for the speed of sound in seawater. J Acoust Soc Am 32(10):1357

Zheng J, Liu B, Kan G, Li G, Pei Y, Liu X (2016) The sound speed and bulk properties of sediments in the Bohai Sea and the Yellow Sea of China. Acta Oceanol Sin 35(7):76–86

Zhong Y, Chen Z, Li L, Liu J, Li G, Zheng X, Wang SH, Mo AB (2017) Bottom water hydrodynamic provinces and transport patterns of the northern south china sea: evidence from grain size of the terrigenous sediments. Cont Shelf Res 140:11–26

Zou DP, Wu BH, Lu B (2011) Seafloor deposition state based geoacoustic model of the South China Sea. Mar Georesour Geotechnol 29(1):61–75